MODE MATCHING ANALYSIS OF A NEW OMNI-DIRECTIONAL CIRCULAR ROD ANTENNA WITH DOUBLE DIELECTRIC GRATINGS FOR MILLIMETER-WAVE APPLICATION*

JING Heng-Zhen XU Shan-Jia

(Department of Electronics Engineering and Information Science, USTC, Hefei, Anhui 230027, China)

Abstract The radiation characteristics of a new millimeter-wave omnidirectional circular rod antenna with double dielectric gratins are analyzed with the rigorous mode matching method. The results indicate that under the condition of the same radiation intensity, the double grating antenna has relatively smaller dimensions than that of the single one. It is undoubtedly a great importance in the case where the limitation of the weight and volume of system is strictly required. The effectiveness and reliability of the present analysis are verified by the related results given in the literature.

Key words double dielectric gratings, MMW, omnidirectional circular rod antenna, mode matching analysis.

新型双介质栅毫米波棒形全向天线的模匹配分析*

靖恒珍 徐善驾

(中国科技大学电子工程与信息科学系,安徽,合肥 230027)

摘要 采用严格的模匹配方法分析了新型双介质栅毫米波棒形全向天线的辐射特性.结果表明,在辐射条件相同的情况下,双栅天线比单栅天线有更小的几何尺寸.这在对系统的重量和体积有严格限制的应用场合无疑具有重要意义.文中所得的结果与文献中相关数据的比较证明了本文分析的有效性和可靠性.

关键词 双介质栅,毫米波,棒形全向天线,模匹配方法分析.

INTRODUCTION

The millimeter-wave region is increasingly being utilized for various systems that generate a need for new types of antennas, including omnidirectional antennas, to suit the various constraints. However even at lower microwave frequencies very few papers have been published on omnidirectional antennas [1~3]. In 1986, an omnidirectional periodic rod leaky-wave antenna structure was proposed [4]. The practicality of the antenna and the effectiveness of the rigorous theory developed in [4] have been justified and confirmed by the practical measurements [5]. The experimental investigation demonstrates that the antenna structure has many advantages, such as wide operating band, simple structure, easy for design and fabrication, scanable electronically by constant of the omnidirectional antenna presented in [5] is small so that a long antenna is required for getting reasonable high efficiency. To improve this performance, a new omnidirectional rod

* The project supported by the National Natural Science Foundation of China (No. 60171019) and Foundation of the Ministry of Education (No. 20010358009)
Received 2002 - 07 - 07, revised 2003 - 01 - 03

* 国家自然科学基金(批准号 60171019)和教育部基金(批准号 20010358009)资助项目
稿件收到日期 2002 - 07 - 07, 修改稿收到日期 2003 - 01 - 03

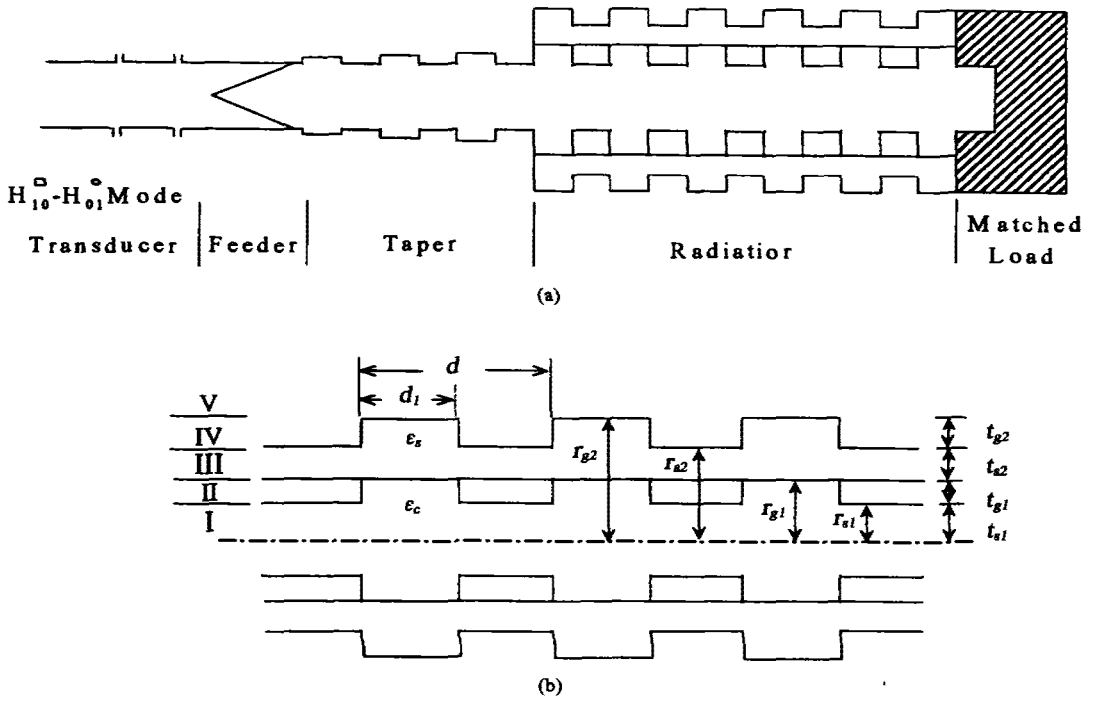

Fig. 1 (a) Configuration of the double gratings antenna (b) Radiator of the double gratings antenna
图 1 (a)双介质栅天线的结构图 (b)双介质栅天线的辐射器

double grating antenna is proposed and analyzed with the rigorous mode matching method in this paper. The results indicate that under the condition of the same radiation intensity, the double grating antenna has relatively smaller dimensions than that of the single one. The theoretical predictions of the leaky characteristics of the present antenna for the case where the thickness of the outer periodic layer is zero are compared with the calculated results given in [6]. The agreement is seen to be very good, and the effectiveness of the theory is thus verified.

1 Theoretical analysis

The schematic of the new omnidirectional circular periodic rod antenna is shown in Fig. 1(a). It consists of several parts, including H_{10}-H_{01} mode transducer, feeder, taper, radiator and matched load.

The radiator of the antenna is shown in Fig. 1 (b), which can be divided into five regions: region Ⅰ, a uniform inner dielectric core; region Ⅱ, a inner circular layer of periodic dielectric medium; region Ⅲ, a circular ring of uniform dielectric medium as shell; region Ⅳ, a outer circular layer of periodic dielectric medium; region Ⅴ, the outer free space. The rod and the inner grating have a relative dielectric constant ε_c, the shell and the outer grating have a relative dielectric constant ε_s. The core, inner grating, shell, outer radii and the period of the corrugation are denoted by r_{s1}, r_{g1}, r_{s2}, s_{g2} and d, respectively as shown in Fig. 1.

The radiation problem of the antenna can be ended into a houndary value problem that is treated by the method of mode matching in this paper. Due to spatial periodicity of the corrugations in the z direction, all the space harmonics are generally excited everywhere in the structure. From Floquet theorem, the electromagnetic fields for the TE_{01} mode exciting can be expressed in matrix form for different regions aas follows:

$$E_\varphi^{(1)} = [J_1(\overline{k_r}^{(1)} r)\exp(-j\overline{k_z} z)]A_1, \quad (1)$$

$$H_z^{(1)} = [\overline{k_r}^{(1)} J_0(\overline{k_r}^{(1)} r)\exp(-j\overline{k_z} z)]A_1/\omega\mu, \quad (2)$$

$$E_\varphi^{(2)} = \overline{V_2}\exp(-j\overline{k_z} z)[H_{21}(\overline{k_r}^{(2)} r)A_2 + H_{11}(\overline{k_r}^{(2)} r)B_2], \quad (3)$$

$$H_z^{(2)} = \overline{I_2}\exp(-j\overline{k_z} z)[H_{20}(\overline{k_r}^{(2)} r)A_2 + H_{10}(\overline{k_r}^{(2)} r)B_2], \quad (4)$$

$$E_\varphi^{(3)} = \exp(-j\overline{k_z} z)[H_{21}(\overline{k_r}^{(3)} r)A_3 + H_{11}(\overline{k_r}^{(3)} r)B_3], \quad (5)$$

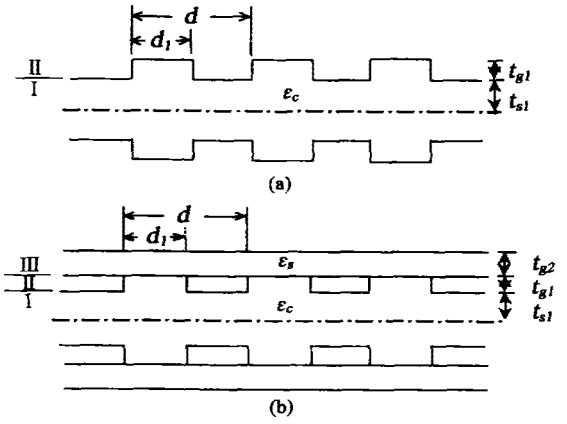

Fig. 2 (a) Radiator of the single grating antenna (b) Radiator of the single grating antenna with shell

图 2 (a)单栅天线的辐射器 (b)带有套筒的单栅天线的辐射器

$$H_z^{(3)} = \overline{k_r^{(3)}}\exp(-j\overline{k_z}z)[H_{20}(\overline{k_r^{(3)}}r)A_3 + H_{10}(\overline{k_r^{(3)}}r)B_3]/\omega\mu, \quad (6)$$

$$E_\varphi^{(4)} = \overline{V_4}\exp(-j\overline{k_z}z)[H_{21}(\overline{k_r^{(4)}}r)A_4 + H_{11}(\overline{k_r^{(4)}}r)B_4], \quad (7)$$

$$H_z^{(4)} = \overline{I_4}\exp(-j\overline{k_z}z)[H_{20}(\overline{k_r^{(4)}}r)A_4 + H_{10}(\overline{k_r^{(4)}}r)B_4], \quad (8)$$

$$E_\varphi^{(5)} = [H_{21}(\overline{k_r^{(5)}}r)\exp(-j\overline{k_z}z)]A_5, \quad (9)$$

$$H_z^{(5)} = [\overline{k_r^{(5)}}H_{20}(\overline{k_r^{(5)}}r)\exp(-j\overline{k_z}z)]A_5/\omega\mu. \quad (10)$$

where $A_i(i=1,2,3,4,5)$ and $B_i(i=2,3,4)$ are infinite column vectors; $\overline{V_i}(i=2,4)$ and $\overline{I_i}(i=2,4)$ are respectively the voltage and current harmonic amplitude matrices; H is the Hankel function, the first subscript stands for the kind order of the function and the second one denotes the order number of the function; $\overline{k_r^{(i)}}(i=1,2,3,4,5)$ and $\overline{k_z}$ are diagonal wavenumber matrices.

At the three interfaces of the inner periodic layers, ($r=r_{s1}$ *and* r_{g1}), the shell layer, (r, r_{g1} and r_{s2}) and the outer periodic layers($r=r_{s2}$ and r_{g2}). the tangential field components must be continuous. Utilizing the general solutions of the five constituent regions to the boundary conditions at the related interfaces result in a system of homogeneous linear equations for the mode amplitudes as follows:

$$[\overline{R}]\begin{pmatrix}A_3\\B_3\end{pmatrix} = \begin{bmatrix}\overline{R}_{11} & \overline{R}_{12}\\ \overline{R}_{21} & \overline{R}_{22}\end{bmatrix}\begin{pmatrix}A_3\\B_3\end{pmatrix} = 0. \quad (11)$$

where

$$\overline{R}_{11} = T_4T_3^{-1}H_{21}(\overline{k_r^{(3)}}r_{g1}) - k_r^{(3)}H_{20}(\overline{k_r^{(3)}}r_{g1}), \quad (12)$$

$$\overline{R}_{12} = T_4T_3^{-1}H_{11}(\overline{k_r^{(3)}}r_{g1}) - k_r^{(3)}H_{10}(\overline{k_r^{(3)}}r_{g1}), \quad (13)$$

$$\overline{R}_{21} = S_4S_3^{-1}H_{21}(\overline{k_r^{(3)}}r_{s2}) - k_r^{(3)}H_{20}(\overline{k_r^{(3)}}r_{s2}), \quad (14)$$

$$\overline{R}_{22} = S_4S_3^{-1}H_{11}(\overline{k_r^{(3)}}r_{s2}) - k_r^{(3)}H_{10}(\overline{k_r^{(3)}}r_{s2}). \quad (15)$$

and

$$T_3 = \overline{V_2}[H_{21}(k_r^{(2)}r_{g1}) - H_{11}(k_r^{(2)}r_{g1})T_2^{-1}T_1], \quad (16)$$

$$T_4 = \overline{I_2}[H_{20}(k_r^{(2)}r_{g1}) - H_{10}(k_r^{(2)}r_{g1})T_2^{-1}T_1], \quad (17)$$

$$S_3 = \overline{V_4}[H_{21}(k_r^{(4)}r_{s2}) - H_{11}(k_r^{(4)}r_{s2})S_2^{-1}S_1], \quad (18)$$

$$S_4 = \overline{I_4}[H_{20}(k_r^{(4)}r_{s2}) - H_{10}(k_r^{(4)}r_{s2})S_2^{-1}S_1]. \quad (19)$$

here

$$T_1 = \overline{k_r^{(1)}}J_0(\overline{k_r^{(1)}}r_{s1})\,\overline{V_2}H_{21}(\overline{k_r^{(2)}}R_{s1}) - J_1(\overline{k_r^{(1)}}r_{s1})\,\overline{I_2}H_{20}(\overline{k_r^{(2)}}r_{s1}), \quad (20)$$

$$T_2 = \overline{k_r^{(1)}}J_0(\overline{k_r^{(1)}}r_{s1})\,\overline{V_2}H_{11}(\overline{k_r^{(2)}}R_{s1}) - J_1(\overline{k_r^{(1)}}r_{s1})\,\overline{I_2}H_{10}(\overline{k_r^{(2)}}r_{s1}), \quad (21)$$

$$S_1 = H_{21}(\overline{k_r^{(5)}}r_{g2})\,\overline{I_4}H_{20}(\overline{k_r^{(4)}}r_{g2}) - \overline{k_r^{(5)}}H_{20}(\overline{k_r^{(5)}}r_{g2})\,\overline{V_4}H_{21}(\overline{k_r^{(4)}}r_{g2}), \quad (22)$$

$$S_2 = H_{21}(\overline{k_r^{(5)}}r_{g2})\,\overline{I_4}H_{10}(\overline{k_r^{(4)}}r_{g2}) - \overline{k_r^{(5)}}H_{20}(\overline{k_r^{(5)}}r_{g2})\,\overline{V_4}H_{11}(\overline{k_r^{(4)}}r_{g2}). \quad (23)$$

The existence of a nontrivial solution for (11) requires that the coefficient determinant vanish:

$$\mathrm{Det}([\overline{R}]) = 0. \quad (24)$$

The determinant equation (24) defines the dispersion relation, from which the complex eigenvalue $k_z = \beta - j\alpha$ then the radiation characteristics of the antenna can be completely determined.

2 Numerical results

In order to quantify the leaky characteristics of the present antenna the developed model is applied to generate a large amount of numerical results involving parametric effects. Since for antenna applications, one is interested mostly in the case of a single beam radiation. The case where only $n = -1$ space harmonic of TE_{01} mode radiates into free space is investigated here.

Fig. 3 shows the variations of the normalized leakage constant α/k_0 with the normalized periodic layer thickness t_{g1}/λ for the single grating antenna with shell shown in Fig. 2(b), with the core radius as a parameter. The solid line represents theoretical predictions for the double grating antenna with the outer periodic layer thickness being zero using the present procedure, while, the symbols · indicate the theoretical data presented in [6]. From the figure, very good agreement has been found; the effectiveness of the present analy-

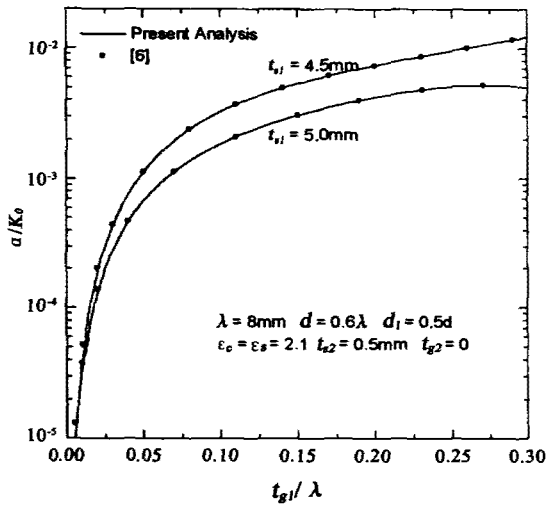

Fig. 3 Effect of grating layer thickness t_{g1}/λ on leakage constant for the single grating antenna with shell.

图3 栅层厚度 t_{g1}/λ 对带有套筒的单栅天线漏波常数的影响

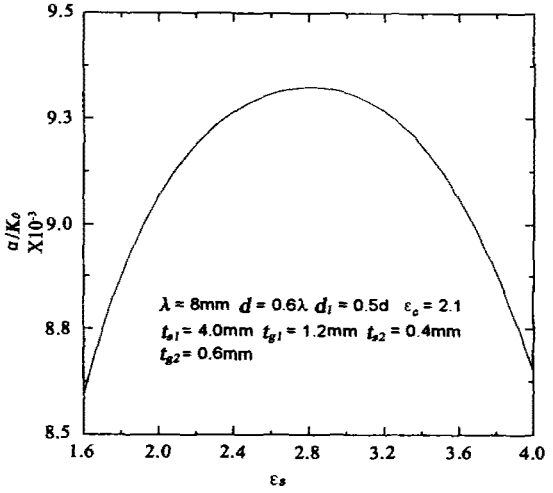

Fig. 5 Variation of the normalized leakage constant α/k_0 with ε_s for double grating antenna

图5 归一化漏波常数 α/k_0 随双栅天线 ε_s 的变化

sis is thus justified.

Fig. 4 shows the variations of the normalized leakage constant α/k_0 with the normalized periodic layer thickness t_{g1}/λ for three type of antennas. In order for comparison, the same overall size of these antennas are chosen. The radiators of the three type of antennas are shown in Fig. 1(b), Fig. 2(a) and Fig. 2(b) respectively. The structure parameters are given in the insets of the figure. It is seen from the figure that the leakage constant α of the double grating antenna is larger than of the single one with and without shell, in the whole region of t_{g1} calculated, because of the strong perturbation effect on guided wave caused by the two grating antenna layers. It means that under the condition of the same radiation strength, the length of the double grating antenna can be considerable reduced compared with the single one with and without shell.

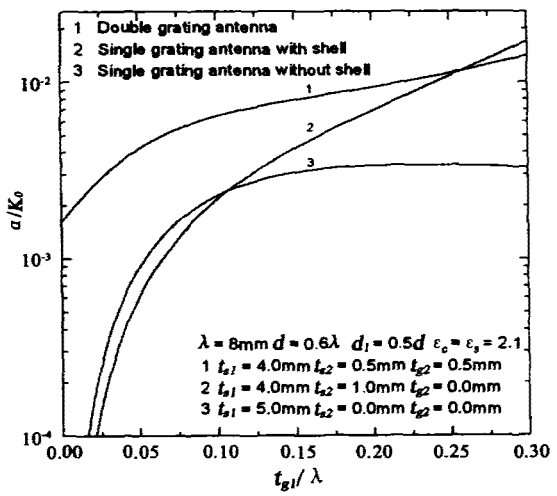

Fig. 4 Effect of grating layer thickness t_{g1}/λ on leakage constant for three types of antennas.

图4 栅层厚度 t_{g1}/λ 对三种介质栅天线漏波常数的影响

It is found from Fig. 4 that the leakage constant of the single grating antenna with shell increases more rapidly as the thickness tg_1 increases than the one without shell. The reason for this is that the shell layer makes the fields of the surface wave concentrate within the grating layer, so that the perturbation effect on guided wave has been strengthened prominently.

Fig. 5 shows the variations of the leakage constant with the dielectric constant of the outer grating layer, which varies from 1.6 to 4.0. When the dielectric constant of the outer grating layer is small, the leakage constant increases with the increment of the dielectric constant ε_s. This is because the larger ε_s makes the fields of the surface wave concentrated in the inner grating layer and the perturbation effect on guided wave is strengthened. However, as the dielectric constant is increased further from 2.8, the leakage decreases. The reason for that is as ε_s increases further, the fields of surface wave enters the shell, in this case the fields in the inner grating layer becomes weaker, so does the leakage.

Fig. 6 shows the variations of the 3-dB beamwidth

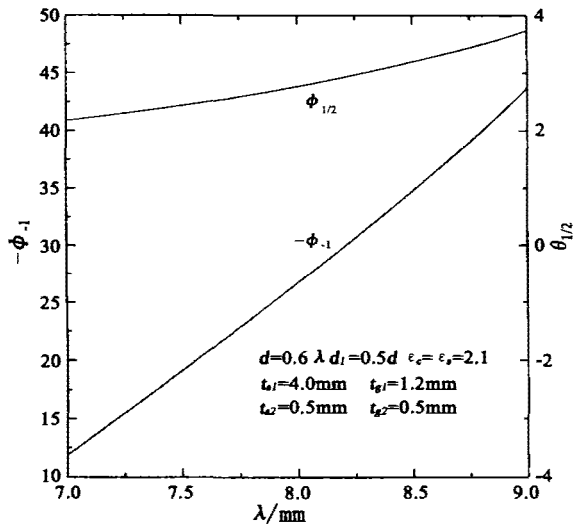

Fig. 6　Frequency scanning characteristics of the double gratings antenna

图 6　双栅天线的频率扫描特性

$\theta_{1/2}$ in the H-plane and the maximum radiation angle θ_{-1} with the wavelegth for the double grating antenna shown in Fig. 1 (b). The physical parameters are shown in the insets. It is found from Fig. 6 that the double grating antenna maintains the advantages of the original antenna presented in ref. [6], that is the main beam sweeps almost linearly over angular range from 12° to 43°, whereas the 3-dB beamwidth only changes almost linearly from 2. 2° to 3. 8°. It is a desirable property for practical use as a frequency scanning antenna, since it ensures a stable radiation pattern with little distortions as beam is being scanned.

3 Summary

A new millimeter-wave omnidirectional circular rod antenna with double dielectric gratings is proposed and the radiation characteristics of the antenna are analyzed with the rigorous mode matching method. Extensive mumerical results are given for design of the antenna. The results indicate that under the condition of the same radiation intensity, the double grating antenna has relatively smaller dimension than that of the single one. It is undoubtedly of great importance in the case where the limitation of the weight and volume of system is strictly required. The effectiveness and reliability of the present analysis are verified by the related results given in the literature.

REFERENCES

[1] Hill R. A twin line omni-directional aerial configuration. In: *8th European Microwave Conf. Rec.*, *Sep.*, 1978, 307

[2] Krall A D, McCorkle J M, Scarzello J F, *et al.* The omni microstrip antenna: A new small antenna, *IEEE Trans. on Antennas Propagat.*, 1979, **27**: 850

[3] Volta P. Design and development of an omnidirectional antenna with a colline array of slots. *Microwave J.*, 1982, 111

[4] Peng S T, Xu Shanjia, Schwering F K. Omnidirectional periodic rod antenna. *IEEE Antennas Propagat. Soc. Int. Symp. Dig.*, 1986, 697

[5] Xu Shanjia, Min Jianhua, Peng S P, *et al.* A millimeter wave omni-directional circular dielectric rod grating antenna. *IEEE Trans. on Antennas Propagat.*, 1991, **39**: 883

[6] Jing Hengzhen, Xu Shanjia. Mode Matching Analysis for a New Millimeter Wave Omni-Directional Antenna Consisting of Circular Rod Corrugations Gloved with a Dielectric Shell. (Submitted to *IEEE Transactions on antennas and propagation*)

[7] MAO Kai-Yu, XU Shan-Jia. Analysis for transmission characteristics of non-uniform dielectric waveguides with arbitrarily transverse cross-sections. *J. Infrared milli. waves* (毛开宇,徐善驾. 任意横截面形状非均匀介质波导传输特性的分析. **红外与毫米波学报**), 2002, **21**(6): 434—438

[8] DONG Jian-Feng, XU Shan-Jia. Reflection and Transmission of coaxial waveguide partially filled with chiral media. *J. Imfrared milli. waves* (董建峰,徐善驾. 部分手征介质填充同轴线的反射和透射特性. **红外与毫米波学报**), 2002, **21**(5): 356—360

[9] ZHOU Ping, XU Shan-Jia. The application of 3-D PML absorbing boundary conditions to the analysis of microstrip discontinuities. *J. Infrared milli. waves* (周平,徐善驾. 三维PML吸收边界条件在微带线不连续性问题分析中的应用. **红与毫米波学报**), 2001, **20**(6): 451—454